REGULAR ARTICLE

blood advances

Interferon gamma rebalances immunopathological signatures in chronic granulomatous disease through metabolic rewiring

Mariolina Bruno,[1] Charlotte Kröger,[2,3] Anaísa V. Ferreira,[1] Bowen Zhang,[4-6] Rutger J. Röring,[1] Ruiqi Liu,[1] Caspar I. van der Made,[1] Norman van Rhijn,[7] Laszlo Groh,[1] Viola Klück,[1] Nico A. F. Janssen,[1] Wenchao Li,[4,5] Diletta Rosati,[1] Ahmed Alaswad,[4,5] Helin Tercan,[1] Jorge Saiz,[8] Carolina Gonzalez-Riano,[8] Martina van Uelft,[2,3] Orsolya Ildiko Gaal,[1,9] Sophie Müller,[2,3,10] Humberto J. Ferreira,[11,12] Stefanie Warnat-Herresthal,[2,3] Matthias Becker,[3] Lisa Holsten,[2,3] Michael Kraut,[3,11] Jonas Schulte-Schrepping,[2,3,11] Lorenzo Bonaguro,[2,3,11] Kristian Händler,[3,11,13] Cristina Cunha,[14,15] Manfred Schmolz,[16] Joachim L. Schultze,[2,3,11] Leo A. B. Joosten,[1,11] Coral Barbas,[8] Mihai G. Netea,[1,2] Yang Li,[1,4,5] Anna C. Aschenbrenner,[3] Agostinho Carvalho,[14,15] and Frank L. van de Veerdonk[1]

[1]Department of Internal Medicine and Radboudumc Community for Infectious Diseases, Radboud University Medical Center, Nijmegen, The Netherlands; [2]Department for Genomics & Immunoregulation, Life and Medical Sciences Institute, University of Bonn, Bonn, Germany; [3]Deparment of Systems Medicine, Deutsches Zentrum für Neurodegenerative Erkrankungen, Bonn, Germany; [4]Department of Computational Biology for Individualised Medicine, Centre for Individualised Infection Medicine, a joint venture between the Hannover Medical School and the Helmholtz Centre for Infection Research, Hannover, Germany; [5]TWINCORE, Centre for Experimental and Clinical Infection Research, a joint venture between the Hannover Medical School and the Helmholtz Centre for Infection Research, Hannover, Germany; [6]Key Laboratory for Biodiversity Science and Ecological Engineering, College of Life Sciences, Beijing Normal University, Beijing, China; [7]Microbial Evolution Research Manchester, Division of Evolution, Infection and Genomic Sciences, Faculty of Medicine, Biology and Health, The University of Manchester, Manchester, United Kingdom; [8]Chemistry and Biochemistry Department, Pharmacy Faculty, Centre for Metabolomics and Bioanalysis, Universidad San Pablo-CEU, CEU Universities, Madrid, Spain; [9]Department of Medical Genetics, Iuliu Haţieganu University of Medicine and Pharmacy, Cluj-Napoca, Romania; [10]Department of Microbiology and Immunology, The University of Melbourne at the Peter Doherty Institute for Infection and Immunity, Melbourne, VIC, Australia; [11]PRECISE Platform for Single Cell Genomics and Epigenomics, Deutsches Zentrum für Neurodegenerative Erkrankungen and University of Bonn, Bonn, Germany; [12]Department of Oncology, Centre Hospitalier Universitaire Vaudois, Lausanne, Switzerland; [13]Institute of Human Genetics, Universitätsklinikum Schleswig-Holstein, University of Lübeck and University of Kiel, Lübeck, Germany; [14]Life and Health Sciences Research Institute, School of Medicine, University of Minho, Braga, Portugal; [15]ICVS/3B's - PT Government Associate Laboratory, Braga/Guimarães, Portugal; and [16]HOT Screen GmbH, Reutlingen, Germany

Key Points

- CGD monocytes exhibit profound glycolytic and mitochondrial metabolic defects, and reduced intracellular amino acid levels.
- IFN-γ rebalances metabolic and functional defects in CGD monocytes, revealing mechanisms behind its prophylactic benefits in CGD.

Chronic granulomatous disease (CGD) is a primary immunodeficiency characterized by recurrent life-threatening infections and hyperinflammatory complications. It is caused by mutations in the reduced nicotinamide adenine dinucleotide phosphate (NADPH) oxidase complex and the consequent loss of reactive oxygen species (ROS) production. Recombinant human interferon gamma (rIFN-γ) prophylaxis reduces the risk of severe infections, but the mechanisms behind its efficacy in CGD are still an open question, as it does not restore NADPH oxidase-dependent ROS production. Here, we demonstrate that the innate immune cells of patients with CGD are transcriptionally and functionally reprogrammed to a hyperactive inflammatory status, displaying an impaired in vitro induction of trained immunity. CGD monocytes have reduced intracellular amino acid concentrations and profound functional metabolic defects, both at the level of glycolysis and mitochondrial respiration. Ex vivo and in vivo treatments with IFN-γ restored these metabolic defects and reduced excessive interleukin 1β (IL-1β) and IL-6 production in response to fungal stimuli in CGD monocytes. These data suggest that prophylactic rIFN-γ modulates the metabolic status of innate immune cells in CGD. These data shed light on the effects of NADPH oxidase–derived ROS deficiency to the metabolic programs of immune

Submitted 12 February 2025; accepted 19 June 2025; prepublished online on *Blood Advances* First Edition 17 July 2025. https://doi.org/10.1182/bloodadvances.2025016213.

Single-cell RNA sequencing (scRNA-seq) data and assay for transposase-accessible chromatin sequencing data have been deposited in the European Genome-phenome Archive (EGA) (accession numbers EGAS00001005463 and EGAS00001005915, respectively). Bulk RNA-seq aligned reads can be accessed through BioProject ID PRJNA1123445.

Original data and resources are available on request from the corresponding authors, Mariolina Bruno (mariolina.bruno@radboudumc.nl) and Frank L. van de Veerdonk (frank.vandeveerdonk@radboudumc.nl).

The full-text version of this article contains a data supplement.

cells and pose the basis for targeting this immunometabolic axis, potentially beyond CGD, with IFN-γ immunotherapy.

Introduction

Chronic granulomatous disease (CGD) is a rare inherited immunodeficiency with an estimated frequency of 1:200 000 to 1:250 000 in newborns.[1] Distinct causative genetic mutations have previously been defined in the 5 genes encoding the subunits of the reduced NAD phosphate (NADPH) oxidase complex,[1] which is mainly expressed in mononuclear phagocytes and granulocytes,[2] with additional expression in T, B,[3] and endothelial cells.[4] The NADPH is a multicomponent protein complex composed of the $p22^{phox}$, $gp91^{phox}$, $p47^{phox}$, $p67^{phox}$, and $p40^{phox}$ subunits. The $p22^{phox}$ and $gp91^{phox}$ subunits are transmembrane proteins and couple with the cytosolic subunits ($p47^{phox}$, $p67^{phox}$, and $p40^{phox}$) and the small guanosine triphosphate (Rac1 and Rac2) on cell activation. This activation leads to the transfer of electrons from cytosolic NADPH to intraphagosomal or extracellular oxygen and results in the generation of oxygen superoxide, a potent reactive oxygen species (ROS).[3] Owing to mutations in the NADPH oxidase complex, patients with CGD display a severe deficiency in NADPH oxidase-dependent ROS production. The main symptoms of patients with CGD include life-threatening recurrent bacterial and fungal infections, hyperinflammatory complications such as colitis, multisystemic granuloma formation, and increased risk of autoimmune disease.[5] An altered transcription of proinflammatory mediators, a more highly active caspase-1 (p10) expression in unstimulated monocytes,[6] and defective autophagy in macrophages[7] have been established as part of the hyperinflammatory phenotype. Appropriate antibiotic and antifungal prophylaxis is crucial in preventing patients with CGD from developing serious infections.[8] At present, hematopoietic stem cell transplantation is the only available curative treatment for CGD, with a success rate of 90%,[9] but gene therapy has also been applied successfully.[10] Prophylactic immunotherapy with recombinant human interferon gamma (rIFN-γ) has been found to reduce the relative risk of developing serious infections in patients with CGD by 67%.[11,12] However, the precise biological mechanism behind this protection remains unclear.[13] Here, we reveal that human innate immune cells isolated from patients with CGD display a distinct transcriptional and epigenetic profile compared with the healthy controls and profound functional metabolic defects. Our data define dysregulated immunometabolism with hyperinflammation as a consequence of deficient NADPH oxidase-dependent ROS production in myeloid cells as a new pathophysiological concept in CGD which can be reversed by IFN-γ in a prophylactic regimen.

Materials and methods

Ethics statement and patient material

Healthy volunteers were recruited through a voluntary blood donation platform at Radboud University Medical Center. Approval for including healthy controls was obtained from the Medisch Etische Toetsingscommissie Arnhem-Nijmegen (NL32357.091.10), adhering to International Council for Harmonisation-Good Clinical Practice guidelines. The inclusion of patients with CGD was approved by the Institutional Review Board (National PID study, NL40331.078). EDTA blood was collected from healthy controls (self-reported free of infections) and genetically diagnosed patients with CGD with confirmed impaired ROS production. Buffy coats from healthy donors (Sanquin blood bank) were used for apocynin-related experiments, whereas fresh peripheral blood was used for all other assays. Details on protocols, blood counts, plasma storage, cell culture, and other methods are available in the supplemental Methods.

Single-cell RNA-seq

Peripheral blood was drawn from 5 patients with CGD and 5 matched controls into medium-filled TruCulture tubes. For 4 participants in each group, additional blood samples were collected in IFN-γ–filled tubes. Further processing details are available in the supplemental Methods.

ATAC-seq

Assay for transposase-accessible chromatin sequencing (ATAC-seq) was performed on monocytes from the same subjects used for bulk RNA sequencing (RNA-seq), following a protocol with minor adaptations[14] (supplemental Methods).

Liquid chromatography-mass spectrometry/mass spectrometry–targeted metabolomics and lipidomics sample preparation

Monocytes (2×10^6) and neutrophils (2×10^6) from CGD and control donors were incubated at 37°C for 2 hours. Pellets were frozen in liquid nitrogen to quench metabolism and stored at −80°C. Metabolite extraction was conducted using the methyl tert-butyl ether/methanol/water method. Lipidomics used snap-frozen monocyte pellets (5×10^5 cells per pellet). Further details are provided in the supplemental Methods.

Functional metabolic analysis by Seahorse

Neutrophils (4×10^5) and monocytes (2×10^5) were plated in precalibrated cartridges with assay media (coated with Corning Cell-Tak in the case of neutrophils). Oxygen consumption rate (OCR) and extracellular acidification rate (ECAR) were assessed using Seahorse XF Cell Mito Stress and Glycolysis (Glyco) Stress tests on an XFe96 analyzer. The supplemental Methods include additional experimental details.

Quantification and statistical analysis

In vitro monocyte experiments were performed at least thrice independently, and for each analysis, at least 1 healthy control was included as a reference. Data comparisons were analyzed using Mann-Whitney *U* test for unpaired samples and a Wilcoxon signed-rank test for paired data. A 2-sided *P* value $<.05$ was considered statistically significant. All data from the in vitro experiments with >3 subjects were analyzed using GraphPad Prism 8.0. Data are illustrated as means ± standard error of the mean. Except for the plasma and supernatant proteomic experiment, neutrophil 4-hour

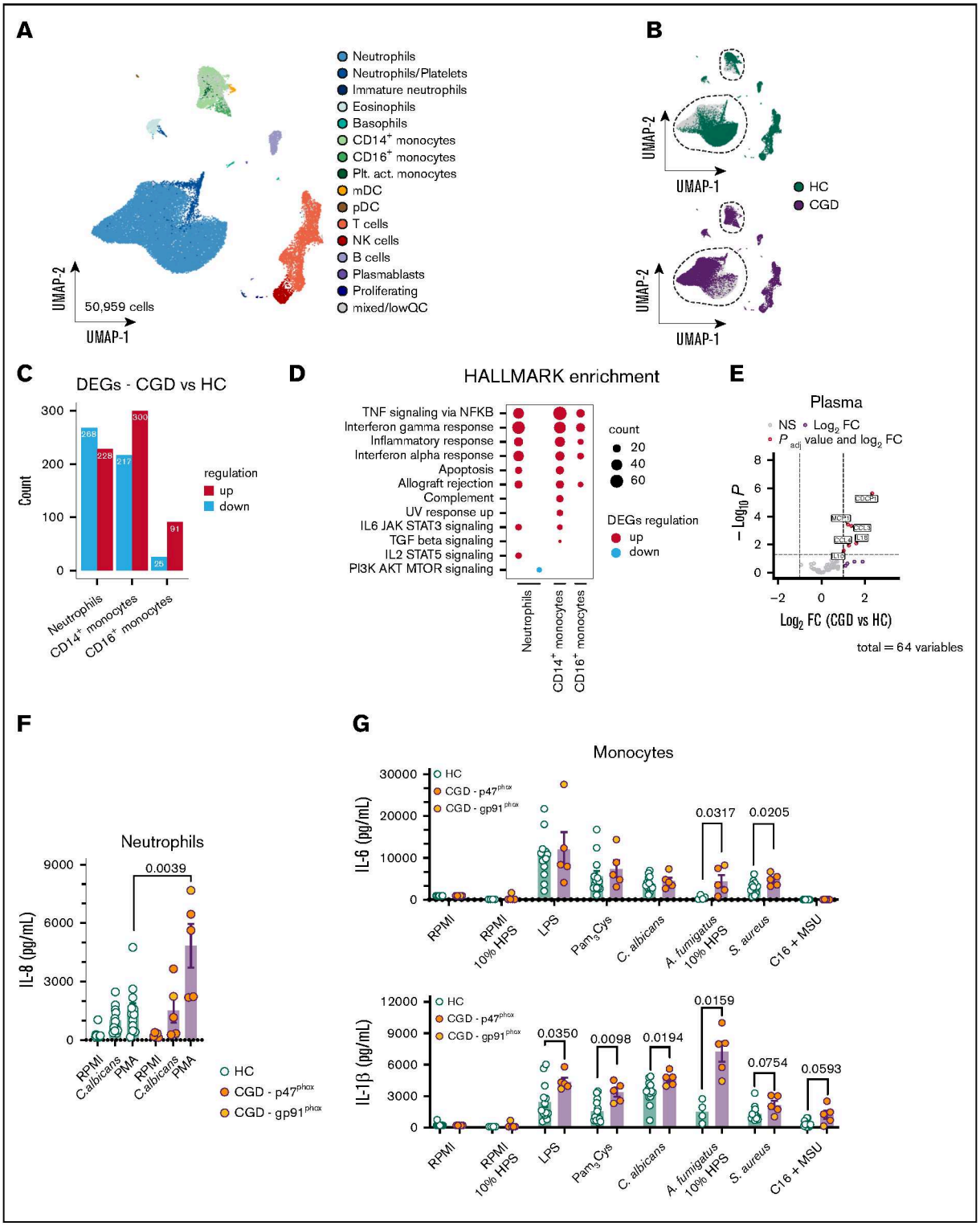

Figure 1. Patients with CGD display a dysregulated hyperinflammatory status. (A) Uniform manifold approximation and projection (UMAP) visualization of scRNA-seq profiles of 50 959 white blood cells from 5 patients with CGD and 5 age- and sex-matched healthy control (HC) colored according to cell type identity. (B) UMAP visualization of cells colored by condition, HC (green) and CGD (purple), downsampled to 3000 cells per donor. (C) Numbers of DEGs identified as upregulated (red) or downregulated (blue) in neutrophils, $CD14^+$ monocytes, and $CD16^+$ monocytes. (D) Gene functional enrichment analysis based on DEGs upregulated or downregulated in neutrophils, $CD14^+$ monocytes, $CD16^+$ monocytes, and neutrophils using HALLMARK gene sets. Illustrated are all significant terms (adjusted $P < .05$). Dots are colored by directionality of differential expression (red, upregulated DEGs; blue, downregulated DEGs). Dot size depicts the number of DEGs in the respective HALLMARK term. (E) Volcano plot of differential abundance of plasma circulatory proteins in patients with CGD (n = 5) as compared with HC (n = 14). Results are displayed as log_2fold change (FC) of CGD compared with HC, plotted against minus

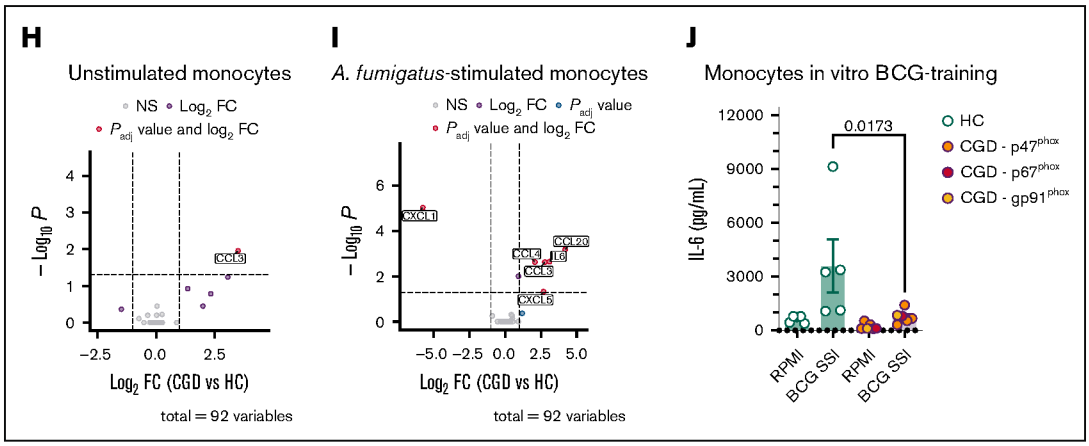

Figure 1 (continued) $\log_{10}$ of the adjusted *P* values. Proteins significantly differentially expressed (with adjusted $P < .05$ after correction for multiple testing) are displayed in red. (F) IL-8 production after 4-hour stimulation in neutrophils from CGD (n = 5) and HC (n = 12) with either medium (RPMI), heat-killed *C albicans* UC820 (1×10^6 yeast per mL), or PMA (50 ng/mL). (G) IL-6 and IL-1β production after 24-hour stimulation in CGD monocytes (n = 5) and HC (n = 13, except for the stimulations RPMI 10% human pooled serum (HPS) and *A fumigatus* where n = 4) with either medium (RPMI, with or without 10% HPS) or LPS (10 ng/mL), Pam_3Cys (10 μg/mL), heat-killed *C albicans* UC820 (1×10^6 yeast per mL), live *A fumigatus* (1×10^6 conidia per mL) in the presence of 10% HPS, *S aureus* ATCC 29213 (1×10^6 colony-forming units per mL), or palmitic acid (C16:0; 50 μM) in combination with monosodium urate crystals (300 μg/mL). (H-I) Volcano plot of differential protein abundance from 24 hour-unstimulated (H) and *A fumigatus*–stimulated (I) Peripheral blood mononuclear cells in culture supernatants of CGD and HC monocytes. Results are displayed as $\log_2$-FC of CGD (n = 5) compared with HC (n = 14), plotted against minus $\log_{10}$ of the *P* values. Proteins with significantly differential abundance (with adjusted $P < .05$ after correction for multiple testing) are displayed in red. (J) IL-6 production after 24-hour LPS (10 ng/mL)-restimulation at day 6 after BCG (5 μg/mL)-training protocol of monocytes from HC (n = 5) and patients with CGD (n = 6). (F-G, J) Data are presented as the means ± standard error of the mean (SEM). In the bar plots, different colors indicate different mutations in patients with CGD as indicated by the panel legends. For the enzyme-linked immunosorbent assay results, statistical analysis was performed using the Mann-Whitney *U* test between patients and HC; a 2-sided *P* value $< .05$ was considered statistically significant. C16, palmitate; MSU, monosodium urate; mDc, myeloid dendritic cells; NK, natural killer; pDC, plasmacytoid dendritic cells; Plt. act., platelet-activated; Pam_3Cys, (*S*)-(2,3-bis(palmitoyloxy)-(2*RS*)-propyl)-*N*-palmitoyl-(*R*)-Cys-(*S*)-Ser(*S*)-Lys_4-OH, trihydrochloride; TNF, tumor necrosis factor.

stimulations, and monocyte 24-hour stimulations, age- and sex-matched healthy controls have been used. For the statistics of proteomics, metabolite analysis, bulk RNA-seq, ATAC-seq, and single-cell RNA-seq (scRNA-seq), details can be found in the dedicated paragraphs and all figure legends.

In vitro monocyte experiments were repeated thrice with at least 1 healthy volunteer as a reference. Data were analyzed with Mann-Whitney *U* tests for unpaired samples and Wilcoxon signed-rank tests for paired samples. A *P* value <.05 was considered significant. Age- and sex-matched controls were used, except in specific cases. Statistical details for proteomics, metabolomics, and sequencing analyses are described in figure legends and the supplemental Materials and methods, whereas scRNA-seq–related figures were generated using ggplot2 (version 3.2.1/3.3.2)[15] and Seurat.

Results

Patients with CGD display a dysregulated inflammatory status

Patients with CGD experience recurrent infections and auto-inflammatory manifestations. To profile potential alterations in the immune system, we analyzed the soluble and cellular components of their blood. Transcriptional differences in blood cell populations from patients with CGD and controls were analyzed by scRNA-seq (Figure 1A). The data set included 50 959 single-cell transcriptomes covering all major blood cell populations (Figure 1A; supplemental Figure 1A; supplemental Table 1). Visualization of the data stratified by disease revealed prominent transcriptional shifts in neutrophils and monocytes (Figure 1B; supplemental Table 1). Differential expression analysis identified the highest number of differentially expressed genes (DEGs) in $CD14^+$ and $CD16^+$ monocytes and mature neutrophils (Figure 1C; supplemental Figure 1B; supplemental Table 1). Enrichment analysis based on HALLMARK gene sets demonstrated the upregulated DEGs in these populations to be enriched in inflammatory response pathways (Figure 1D; supplemental Table 1), and bulk transcriptome analysis from CGD monocytes validated these findings (supplemental Figure 2C). Circulating monocyte counts were higher and basophil counts lower in patients with CGD, as were lymphocyte and basophil percentages (supplemental Figure 1C-D). Six plasma cytokines and chemokines (CDCP1, MCP-1, CCL3, IL-18, CCL4, IL-10) were significantly elevated in patients with CGD (Figure 1E). ROS production in CGD neutrophils was absent following *Candida albicans* or phorbol myristate acetate (PMA) stimulation (supplemental Figure 1E), whereas IL-8 production was increased after PMA stimulation (Figure 1F). CGD monocytes demonstrated heightened proinflammatory responses: stimulation with *Aspergillus fumigatus* triggered higher IL-6 and IL-1β levels; lipopolysaccharide (LPS), Pam_3Cys, and heat-killed *C albicans* stimulation caused elevated IL-1β levels. *Staphylococcus aureus* stimulation led to higher IL-6 and IL-1Ra production (Figure 1G; supplemental Figure 2A). CGD monocytes exhibited higher IL-1β/IL-1Ra ratios, indicating increased IL-1 bioactivity (supplemental Figure 2B). Proteomic analysis of cell supernatants revealed elevated CCL3 production in unstimulated monocytes (Figure 1H) and higher CCL3, CCL4, CCL20, and CXCL5 levels after *A fumigatus* stimulation (Figure 1I). We further tested trained immunity capacity[16] as a measure of innate immune function,

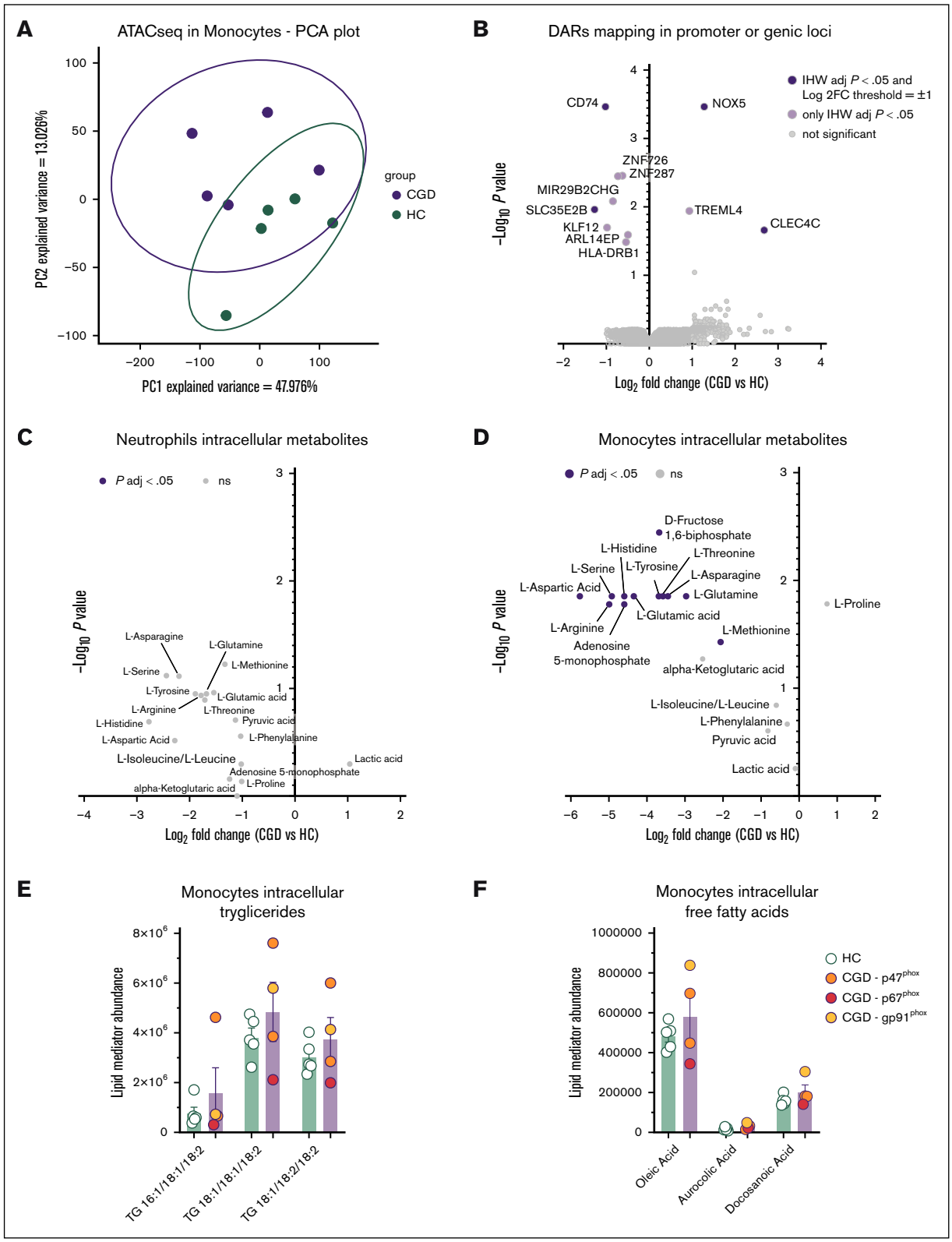

Figure 2. Epigenetic landscape and metabolic profile of CGD monocytes. (A) Principal component analysis of the accessible peaks of unstimulated monocytes from HC (n = 5) and CGD (n = 5) detected with ATAC-seq. The first 2 principal components are visualized, where PC1 accounts for 47.976% of the total variance epigenetic profile. (B) Volcano plot of differentially accessible regions mapping in promoter or genic loci of monocytes from HC (n = 5) and patients with CGD (n = 5) assessed by ATAC-seq. Peaks with an adjusted IHW *P* value <.05 and a mean $log_2FC > 1$ or < -1 are plotted in dark purple. (C-D) Volcano plots of differentially abundant metabolites between neutrophils (C) and monocytes (D) from HC (n = 3) and patients with CGD (n = 5) assessed by targeted metabolomics. The plots represent log_2FC and $-log_{10}$ of the corrected *P* values

which was reduced in CGD macrophages: unlike healthy controls, CGD macrophages failed to increase IL-6 levels after Bacillus Calmette-Guérin (BCG) exposure and LPS restimulation (Figure 1J). These findings align with previous studies revealing heightened proinflammatory cytokine production by neutrophils and mononuclear cells from patients with CGD,[6,17,18] reflecting an activated state.

The disease phenotype in CGD monocytes is not determined by chromatin accessibility changes

To investigate whether the hyperinflammatory state of CGD monocytes stems from changes in the epigenetic landscape, ATAC-seq was performed on circulating monocytes. A principal component analysis revealed a distinct pattern between patients with CGD and healthy controls, with PC1 explaining 47.98% of the variance (Figure 2A). Monocytes from patients with CGD exhibited more accessible regions in intergenic regions and noncoding RNAs (supplemental Figure 3A). Focusing on peaks mapping to promoter regions or genic loci, increased accessibility was observed in the promoters of the calcium-dependent *NOX5* and the C-type lectin *CLEC4C*, whereas decreased accessibility was noted in the promoter of *CD74* and the nucleoside sugar transporter *SLC35E2B* in CGD monocytes (Figure 2B; supplemental Figure 3B-E). These data confirm that CGD monocytes exhibit altered chromatin accessibility compared with healthy controls; however, despite a clear transcriptional inflammatory signature, this was not accompanied by consistent changes in accessibility at proinflammatory gene loci, suggesting that the hyperinflammatory phenotype of unstimulated CGD monocytes is not primarily driven by ATAC-seq–detectable chromatin accessibility alterations.

Reduced levels of major amino acids in CGD-innate immune cells

As inflammatory dysregulation can be based on changes in metabolism,[19] we investigated metabolic changes in CGD innate immune cells. Targeted metabolite analysis revealed a nonsignificant trend toward lower amino acid levels in CGD neutrophils (Figure 2C). In CGD monocytes, significantly reduced levels of aspartic acid, serine, histidine, glutamic acid, tyrosine, threonine, asparagine, glutamine, arginine, and methionine were found (Figure 2D). In addition, CGD monocytes had lower fructose-1,6-bisphosphate and adenosine-monophosphate, along with a nonsignificant trend toward reduced α-ketoglutarate (α-KG) (Figure 2D). No significant differences were observed in intracellular triglycerides (Figure 2E) and free fatty acids (Figure 2F). Bulk RNA-seq analysis of isolated monocytes of patients with CGD vs those of controls revealed significant transcriptional changes in carbohydrate (*GK*, *PFKP*, *PGD*, *RBKS*) and lipid metabolism (*ACAD8*, *DGKE*, *PLIN2*) genes on 4-hour LPS stimulation and higher succinate dehydrogenase B (*SDHB*) expression in the 4-hour unstimulated setting (supplemental Figure 3F). Overall, CGD monocytes, and to a lesser extent neutrophils, exhibit reduced intracellular amino acids.

Innate immune cells from patients with CGD presented functional metabolic defects

To assess whether the deficient induction of trained immunity and the dysregulated transcriptional and metabolomic profile were linked to functional metabolic defects, the bioenergetic status of CGD monocytes and neutrophils was assessed. CGD monocytes demonstrated impaired glycolysis in the Glyco Stress Test, with significantly lower glycolytic capacity and reserve compared with the controls (Figure 3A). The Mito Stress Test revealed a pronounced bioenergetic defect, with significantly lower basal respiration, maximal respiration, and spare respiratory capacity in CGD monocytes (Figure 3B). Real-time bioenergetic flux analysis of CGD neutrophils demonstrated a reduced basal ECAR and a nonsignificant trend for lower glycolysis and glycolytic capacity (Figure 3C). These findings were confirmed by significantly lower basal lactate production in CGD neutrophils (Figure 3D), consistent with downregulated genes in the phosphoinisitide 3-kinase-AKT-mammalian target of rapamycin pathway, a key regulator of glycolysis and trained immunity[20] (Figure 1D). In contrast, CGD neutrophils display higher levels of basal and a nonsignificant trend toward increased maximal respiration (supplemental Figure 4A). In addition, PMA-induced mitochondrial ROS production was elevated in CGD neutrophils, though not statistically significant (supplemental Figure 4B). Overall, patients with CGD exhibit profound metabolic dysregulation in glucose metabolism (both neutrophils and monocytes) and mitochondrial metabolism (monocytes only).

The impaired metabolism of CGD is NADPH oxidase dependent

To investigate whether NADPH oxidase dysfunction contributes to the observed bioenergetic changes in CGD, we first evaluated the effects of pharmacological inhibition of NADPH oxidase on the metabolic profile of resting and stimulated monocytes from healthy individuals in vitro.

Apocynin, a general NADPH oxidase complex inhibitor, was used, which inhibits ROS production[21] (supplemental Figure 4C) at a noncytotoxic concentration (supplemental Figure 4D). Apocynin treatment led to significantly higher intracellular NADPH levels in monocytes compared with dimethyl sulfoxide–treated controls (Figure 3E). Following 6-hour pretreatment with apocynin, both basal ECAR and OCR were reduced, and zymosan-induced increases in ECAR and OCR were also lower (Figure 3F). To investigate the acute metabolic effect of blocking NADPH oxidase-dependent ROS generation, apocynin was directly injected during the assay ~30 minutes before zymosan treatment. Acute stimulation of monocytes with apocynin resulted in an immediate reduction in basal ECAR but not basal OCR. However, the rapid zymosan-dependent increase in ECAR and OCR was strongly inhibited by apocynin (supplemental Figure 4E). Because the Hv-1 proton channel is activated in conjunction with NADPH oxidase[22(p1)], the reduction in ECAR could be expected. Apocynin-treated monocytes also exhibited significantly lower L-glutamic acid levels

Figure 2 (continued) compared with HC. Metabolites with an adjusted *P* value < .05 and a mean $\log_2$FC > 1 or < −1 are plotted in dark purple and were considered as differentially regulated. (E-F) Intracellular quantification of triglycerides (F) and free fatty acid (G) in unstimulated monocytes from HC (n = 5) and patients with CGD (n = 4). (E-F) Data are presented as the means ± SEM and statistical analysis was performed using the Mann-Whitney *U* test between patients and HC; a 2-sided *P* value <.05 was considered statistically significant. FFA, free fatty acid; IHW, independent hypothesis weighting; kbp, kilobase pairs; ns, not significant; TG, triglyceride; TSS, transcription start site; TTS, transcription termination site.

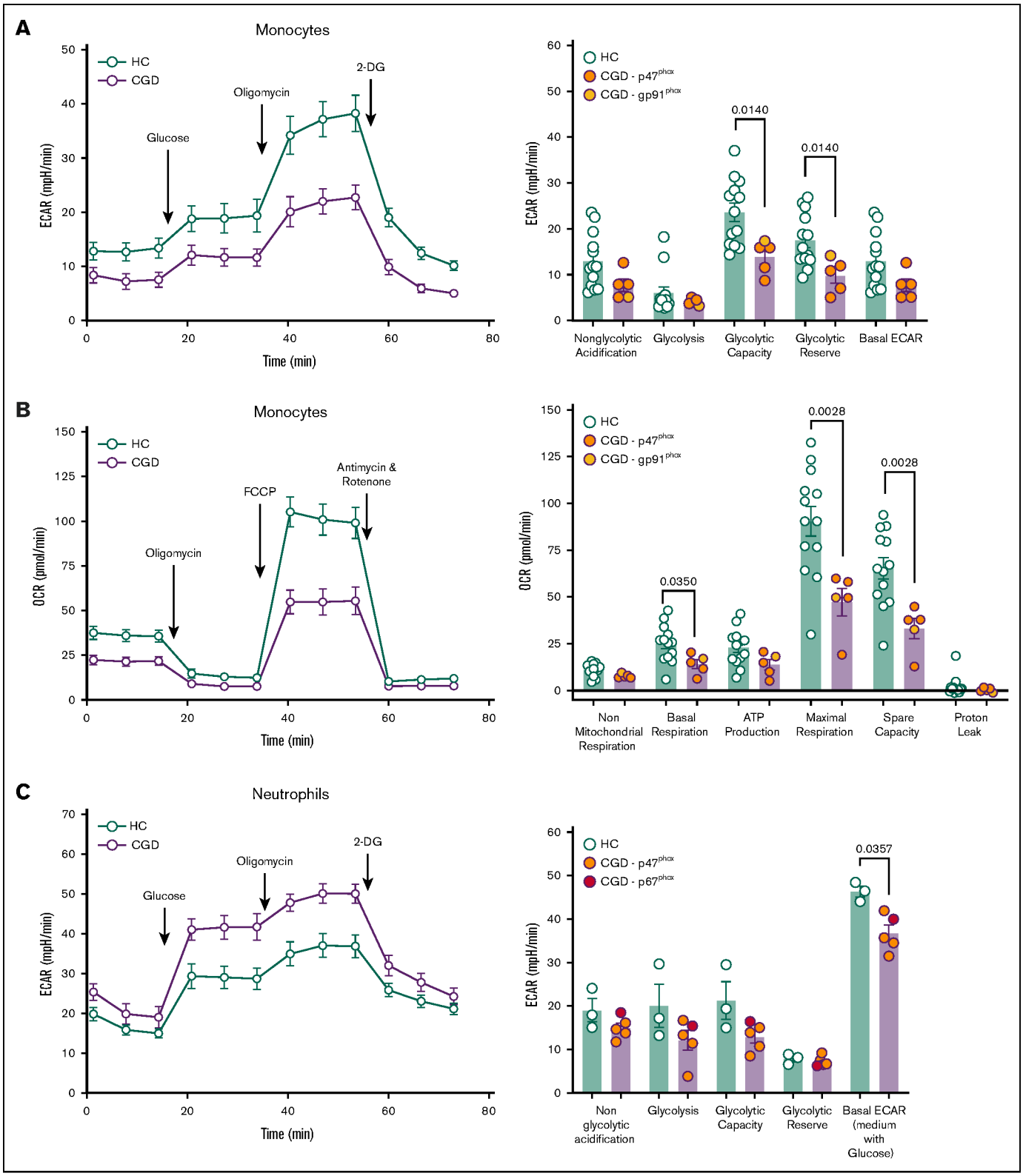

Figure 3. CGD neutrophils and monocytes present functional metabolic defects. (A) ECAR on Glyco Stress Test in monocytes from HC (n = 13) and CGD (n = 5) and relative metabolic glycolytic parameters. (B) OCR on Mito Stress Test in monocytes from HC (n = 13) and patients with CGD (n = 5) relative metabolic mitochondrial parameters. (C) ECAR on Glyco Stress Test in neutrophils from patients with CGD (n = 5) and HC (n = 3) and relative metabolic glycolytic parameters. (D) Lactate production after 4 hours in unstimulated neutrophils from HC (n = 12) and patients with CGD. (E) Intracellular NADPH concentration (pmol/1 000 000 cells) in monocytes of HC (n = 6) incubated for 6 hours with NADPH oxidase complex inhibitor apocynin (1 mM) or its vehicle and stimulated for zymosan for 2 hours. (F) ECAR and OCR after preincubation of monocytes with

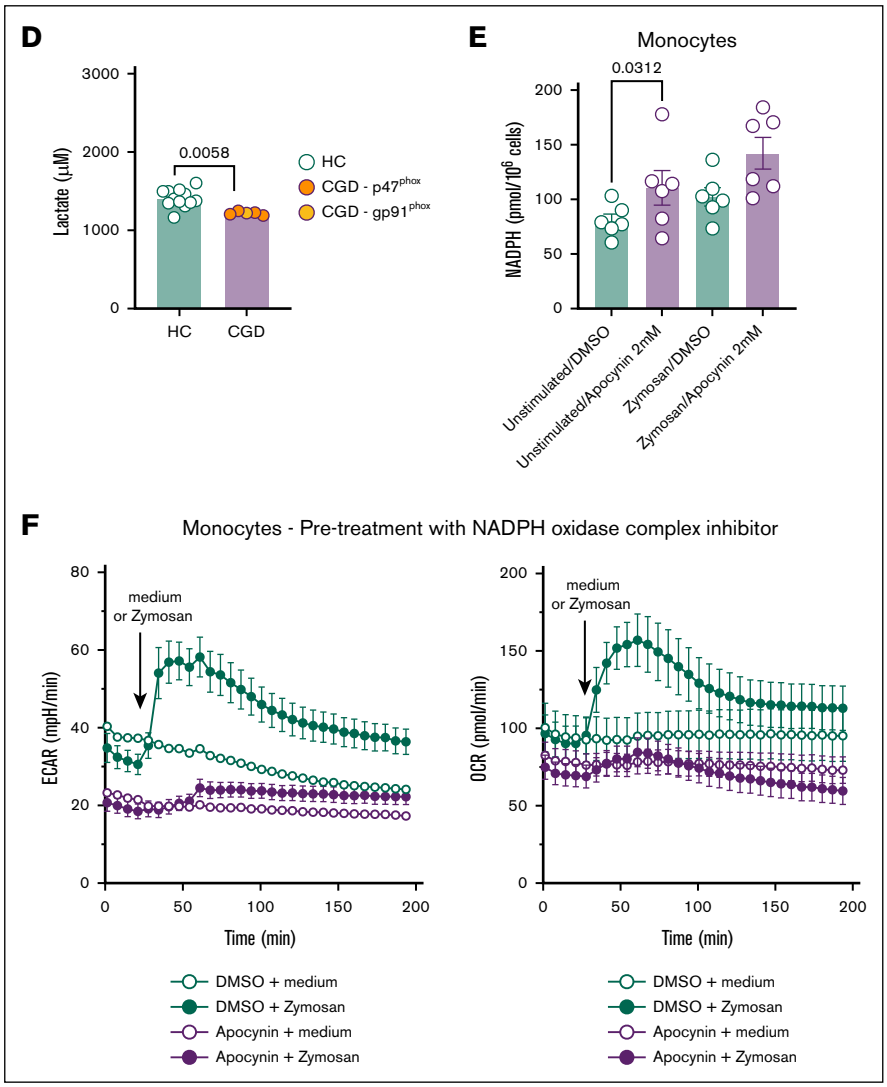

Figure 3 (continued) apocynin (1 mM) for 6 hours followed by stimulation by zymosan (80 µg/mL) during measurements. Data were corrected for background signal of each condition. In the bar plots of panels A-C, different colors indicate different mutations in patients with CGD as indicated by the panel legends. Data are presented as the means ± SEM. Statistical analysis was performed using the Mann-Whitney *U* test between patients and HC; a 2-sided *P* value < .05 was considered statistically significant. DMSO, dimethyl sulfoxide.

(supplemental Figure 4F), similar to the metabolic profile of CGD monocytes (Figure 2D; supplemental Figure 4F). Overall, our in vitro model of NADPH oxidase inhibition with apocynin recapitulates the metabolic changes observed in CGD monocytes, including reduced ECAR/OCR and reduced L-glutamic acid concentrations.

Recombinant IFN-γ treatment restored functional defects in CGD monocytes

We next investigated whether these impaired metabolic pathways observed in CGD immune cells in vitro could be potentially restored by pharmacological treatment. We first tested metformin, which improves cellular bioenergetics[23,24] and influences trained immunity in vitro.[25] Preincubation of monocytes from patients with CGD and healthy controls with metformin did not lead to clear changes in the metabolic phenotype of monocytes from patients with CGD, neither in glycolytic nor mitochondrial metabolism (supplemental Figure 5A-B). Next, we tested rIFN-γ, which is used as antimicrobial prophylaxis for patients with CGD.[11,12] In vitro stimulation of CGD cells with IFN-γ led to a gradual, but transitory, increase of ECAR (supplemental Figure 5C). However, no change in ECAR or OCR was found between treated and untreated CGD monocytes on stimulation with zymosan after direct IFN-γ treatment (supplemental Figure 5C-D). To mimic the prophylactic setting, monocytes from patients with CGD were preincubated with IFN-γ for 12 hours, which resulted in an enhanced glycolytic capacity and glycolytic reserve on Glyco Stress Test (Figure 4A; supplemental Figure 6A) and an improved basal and maximal respiration, spare respiratory capacity, and calculated ATP production on Mito Stress Test (Figure 4B; supplemental Figure 6B). To investigate these effects of IFN-γ at the transcriptional level, we incubated blood samples from patients with CGD and controls directly ex vivo for 4 hours with or without rIFN-γ and performed

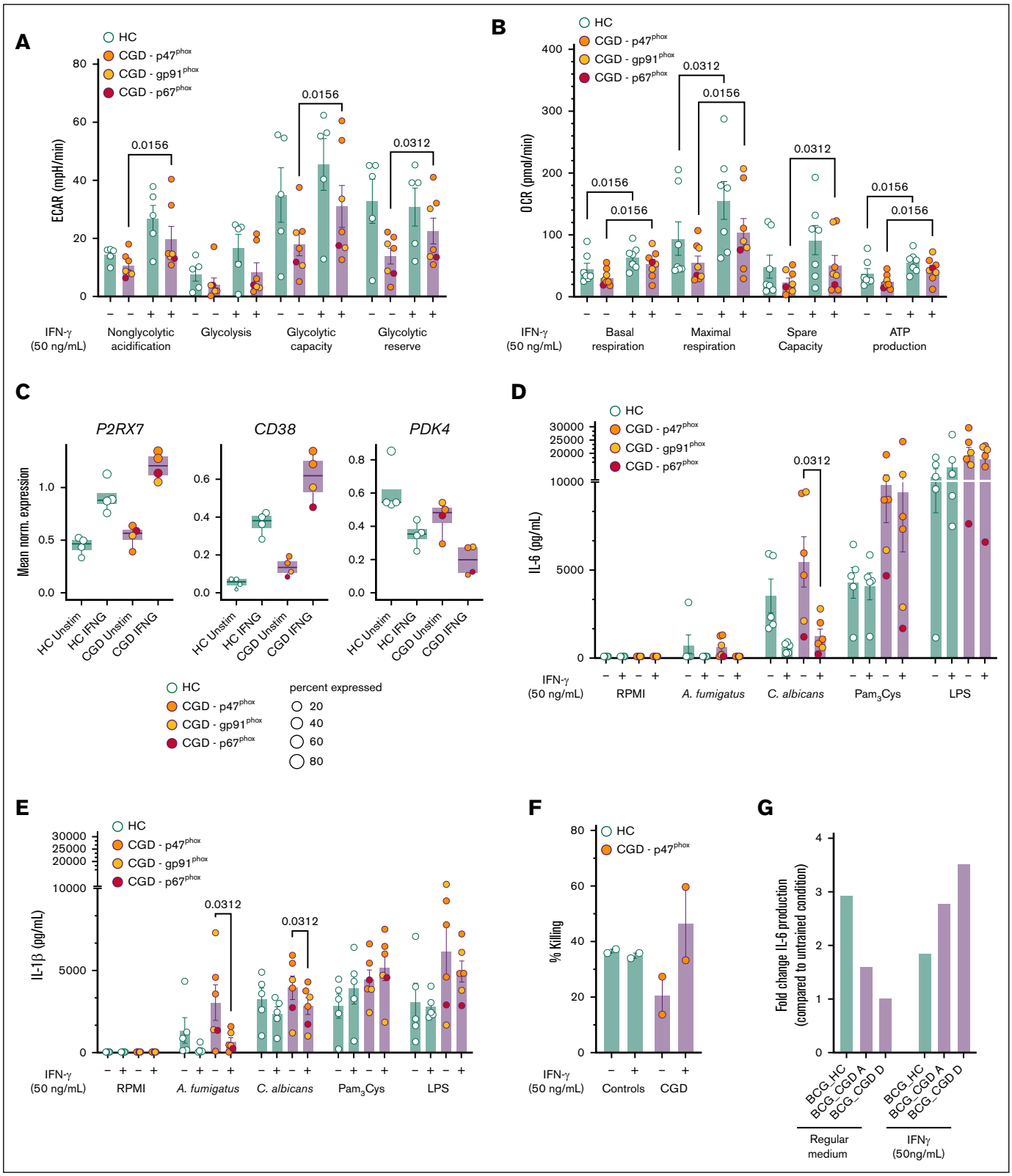

Figure 4. IFN-γ treatment restores functional metabolic defect in CGD monocytes. (A-B) Calculated glycolytic metabolic parameters on the Glyco Stress Test (A) and calculated mitochondrial parameters on Mito Stress Test (B) of monocytes from HC (n = 5 for Glyco Stress Test, n = 7 for Mito Stress Test) and patients with CGD (n = 7 for Glyco Stress Test, n = 8 for Mito Stress Test) after 12 hours treatment with medium (RPMI) or IFN-γ (50 ng/mL) measured by Seahorse XF technology. (C) Mean normalized expression of genes associated with NAD^+ salvage pathway differentially expressed in $CD14^+$ monocytes on 4 hours ex vivo whole blood stimulations with

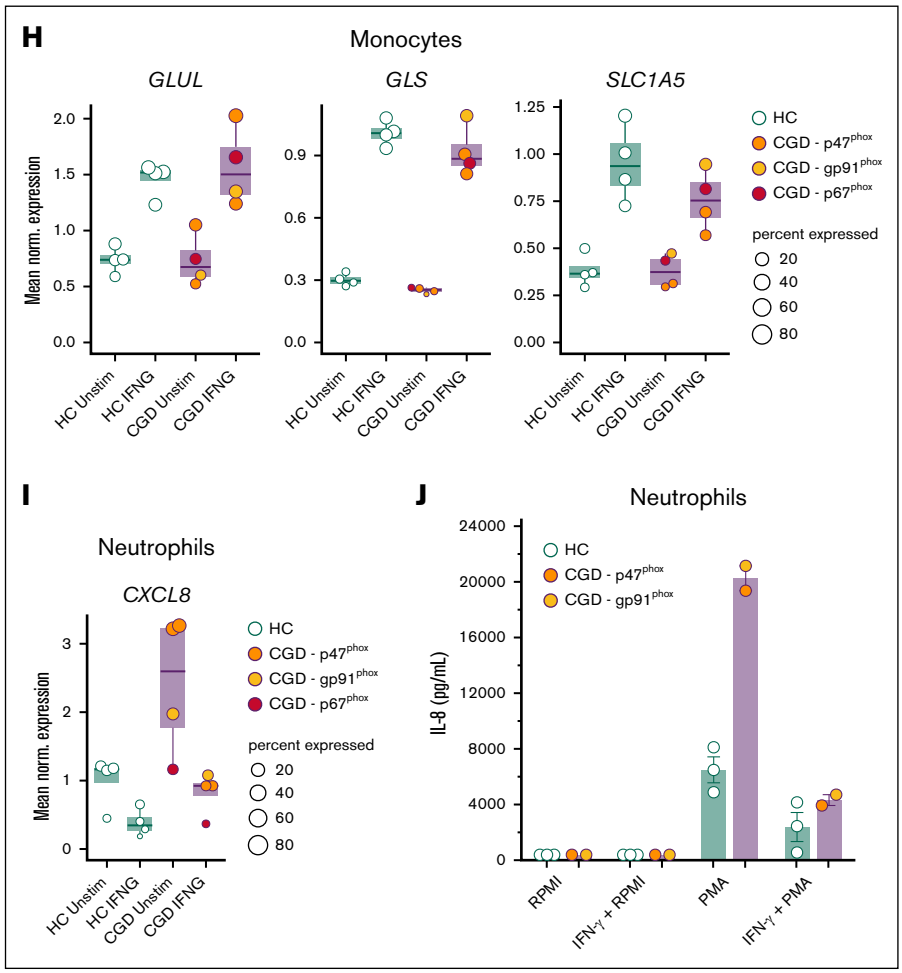

Figure 4 (continued) IFN-γ vs unstimulated within the group of HC (n = 4) and patients with CGD (n = 4), respectively. Dots are colored by donor identity, and dot size is scaled to the percentage of cells expressing the respective gene. (D-E) IL-6 (D) and IL-1β (E) production in CGD monocytes (n = 6) and HC (n = 5) preincubated for 4 hours with or without IFN-γ (50 ng/mL) and then stimulated for 24 hours with either medium (RPMI), live *A fumigatus* (1×10^7 conidia per mL), heat-killed *C albicans* UC820 (1×10^6 yeast per mL), Pam_3Cys (10 μg/mL), or LPS (10 ng/mL). (F) *A fumigatus* outgrowth in monocytes preincubated for 4 hours with or without IFN-γ (50 ng/mL) after the in vitro killing assay, expressed as percentage killing in respect to the total inoculum (CGD n = 2, HC n = 2). (G) Monocytes from HC (n = 1) and patients with CGD (n = 2) were preincubated with IFN-γ (50 ng/mL) and then trained for 24 hours by incubation with 5 μg/mL BCG in the presence of 10% HPS. Thereafter, the stimulus was removed, and cells were kept in RPMI with 10% HPS (regular medium) or in a medium containing 10% human serum and IFN-γ (50 ng/mL). On day 6, a second stimulation with LPS (10 ng/mL) was performed for an additional 24 hours. IL-6 levels were measured in cell culture supernatants after the second stimulation. (H) Mean normalized expression of selected differentially expressed genes related to glutamine metabolism in $CD14^+$ monocytes on 4 hours of ex vivo whole blood stimulation with IFN-γ vs unstimulated within the group of patients with CGD (n = 4) and HC (n = 4), respectively. Dots are colored by donor identity, and dot size is scaled to the percentage of cells expressing the respective gene. (I) Mean normalized gene expression of *CXCL8* in neutrophils on 4 hours of in vitro whole blood stimulation with IFN-γ vs unstimulated demonstrated differential expression in each group (CGD n = 4, HC n = 4) comparing in vitro IFN-γ treated vs untreated cells after 4 hours of incubation. Dots are colored by donor identity, and dot size is scaled to the percentage of cells expressing the respective gene. (J) IL-8 production of HC (n = 3) and CGD neutrophils (n = 2) preincubated for 30 minutes with or without IFN-γ (50 ng/mL) and then stimulated with either medium (RPMI) or PMA (50 ng/mL) for 4 hours. (A, B, D-G, J) Data are illustrated as mean ± SEM, and statistical analysis was performed using the Wilcoxon signed-rank test comparing within the patient group (or within the control group) the IFN-γ–treated condition with the untreated condition.

scRNA-seq. CGD monocytes modulated the transcription of important upstream factors of the NAD^+ salvage pathway, recently described to respond to IFN-γ,[26] including upregulation of *P2RX7* and *CD38* and downregulation of *PDK4* (Figure 4C). Functionally, the aberrant monocyte cytokine production observed in patients with CGD was rebalanced by in vitro preincubation with IFN-γ. *C albicans* induced IL-6, IL-1β, and IL-1Ra production by CGD monocytes after 24 hours, which was significantly reduced as compared with untreated CGD monocytes (Figure 4D-E; supplemental Figure 6C). Moreover, preincubation of CGD monocytes with IFN-γ significantly reduced *A fumigatus*–dependent IL-1β production without affecting IL-1Ra concentrations (Figure 4E; supplemental Figure 6C). *IDO1* and *IL4I1*, important genes of the kynurenine pathway, the latter being dysregulated in CGD,[27] particularly affecting the immune response to *Aspergillus* species,[28,29] were found to be significantly upregulated in CGD monocytes in response to IFN-γ (supplemental Figure 6D). In accordance with this, IFN-γ preincubation improved the defective *A fumigatus* killing capacity specifically of monocytes from 2 patients with CGD (Figure 4F). Furthermore, IFN-γ preincubation

rescued the deficient induction of BCG-trained immunity in CGD (Figure 4G). These findings, although promising, are based on assays conducted in only 2 patients and should be interpreted with caution. Particularly, this restoration may have relied on enhanced glutamine metabolism, known to be crucial for trained immunity[30] and significantly deficient in CGD monocytes (Figure 2D). At the transcriptional level, ex vivo whole-blood IFN-γ stimulation significantly upregulated *GLUL*, *GLS*, and *SLC1A5* in monocytes from both healthy controls and patients with CGD (Figure 4H). Consequently, exogenous L-glutamine supplementation during in vitro induction with BCG, including combined IFN-γ and glutamine, increased LPS-induced IL-6 production at day 6 in 2 patients with CGD (supplemental Figure 6E). Finally, ex vivo whole-blood IFN-γ stimulation reduced the significant upregulated *CXCL8* expression observed in CGD neutrophils to the level of healthy controls (Figure 4I). Correspondingly, 4-hour stimulation with rIFN-γ also rescued the aberrant PMA-induced IL-8 production by CGD neutrophils (Figure 1K; Figure 4J). Collectively, in vitro IFN-γ treatment restored the dysregulated metabolism of CGD immune cells resulting in improved fungal killing, stronger induction of BCG-trained immunity, and rebalancing of aberrant cytokine production.

Recombinant in vivo IFN-γ treatment rebalances proinflammatory state of CGD immune cells

To investigate the in vivo effects of IFN-γ, we evaluated the transcriptional and functional responses after subcutaneous administration of recombinant IFN-γ (3× per week) in 1 patient with CGD carrying a gp91^{phox} mutation (CGD I; Table 1). First, we performed scRNA-seq of the peripheral blood from the patient with CGD before and 4 hours after receiving immunotherapy resulting in 12 136 single-cell transcriptomes covering all major cell types (Figure 5A; supplemental Figure 6F). Visualization of the treatment condition on the global uniform manifold approximation and projection revealed major transcriptional shifts in neutrophils and monocytes (Figure 5B). Differential expression analysis resulted in >200 upregulated and downregulated genes in neutrophils and almost 400 upregulated and >100 downregulated genes in CD14$^+$ monocytes (Figure 5C). The peripheral in vivo treatment response to the immunotherapy 4 hours postsubcutaneous injection was evident from scoring the expression of the HALLMARK "IFN-γ response" gene set in neutrophils and CD14$^+$ monocytes (Figure 5D). Selected genes for glycolysis (*FBP1*), glutamine metabolism (*GLS* and *SLC1A5*), regulation of cytokine homeostasis (*ATP6V1A* and *ATP6V1B2*), and autophagy (*ATG3*) demonstrated differential regulation in monocytes, supporting the functional changes already found in vitro (Figure 5E). Similar to IFN-γ treatment in vitro, IL-8 production by neutrophils was significantly reduced on stimulation with PMA 4 hours after immunotherapy (Figure 5F). Moreover, CGD monocytes presented a boosted mitochondrial metabolism on Mito Stress testing after in vivo IFN-γ (Figure 5G), as demonstrated by a higher basal and maximal respiration and increased ATP-linked respiration (supplemental Figure 6G). Finally, monocytes isolated after receiving in vivo immunotherapy and trained with BCG released higher concentrations of IL-6 on LPS restimulation (Figure 5H). Taken together and in line with the in vitro findings, in vivo IFN-γ immunotherapy in CGD led to a boosted metabolic profile, modulated the IL-8 production capacity in neutrophils, and enhanced the capacity of BCG to induce trained immunity.

Discussion

CGD is a rare inborn error of immunity characterized by impaired phagocyte function, resulting in impaired host defense against pathogens such as *S aureus* and *Aspergillus*. In addition, patients can develop immune dysregulation, including colitis and multisystemic granuloma formation. The hyperinflammatory phenotype of patients with CGD has so far mainly been linked to reduced ROS production.[5] We revealed that the lack of NADPH oxidase activity results in dysregulated immunometabolism and that these defects can be reproduced in healthy monocytes by in vitro NADPH oxidase inhibition. IFN-γ treatment rebalanced both the immunometabolic alterations and proinflammatory cytokine release by monocytes and neutrophils independently of NADPH oxidase restoration. These results suggest that intracellular metabolic dysfunction due to NADPH oxidase deficiency contributes to hyperinflammation in CGD. This may support the use of IFN-γ in other infections with similar pathophysiology.

This study systematically investigated immunometabolism and function of monocytes and neutrophils in CGD, caused by inherited NADPH oxidase deficiency. Previous studies have revealed that deletion or deficiency of NADPH oxidase subunits causes metabolic defects across cell types and disease models, indicating that these changes directly result from NADPH oxidase dysfunction. For instance, hematopoietic cells from *NOX2*-knockout mice display reduced mitochondrial oxygen consumption and glycolytic flux (−25% and −40%, respectively).[31] *NCF1*-knockout models revealed impaired mitochondrial complex I/III activity,[32] whereas NOX2-deficient THP-1 cells display lower glycolysis and oxidative phosphorylation.[33] Furthermore, NOX2-deficient primary human macrophages and CRISPR-engineered models exhibit mitochondrial dysfunction linked to enhanced NLRP3 inflammasome activation.[34] These findings reinforce that NADPH oxidase loss intrinsically leads to immunometabolic dysregulation. Immune cells from patients with CGD demonstrated increased expression of proinflammatory pathway genes, consistent with previous microarray analyses in CGD monocytes and neutrophils.[35,36] Consequently, these cells exhibited a hyperactivated innate immune response and increased cytokine production on stimulation, as found previously.[37,38] Myeloid cells rely heavily on metabolism during activation, and its dysregulation of metabolism can underlie hyperinflammation.[39] CGD monocytes had reduced intracellular levels of major amino acids, α-KG, and fructose-1,6-bisphosphate, along with functional impairment in glycolysis and mitochondrial OXPHOS. They also demonstrated dysregulated transcription of metabolic genes on LPS stimulation. This metabolic rewiring and depletion of key metabolites parallel findings in murine *NOX2*-deficient leukemic stem cells, where similar alterations correlated with enhanced inflammatory signaling.[31] Monjarret et al[34] observed increased mitochondrial mass, reduced mitochondrial potential, and dysfunction in CGD monocytes, functionally linked to NLRP3 activation. Consistently, we found reduced mitochondrial basal and maximal respiration in CGD monocytes, likely tied to intracellular amino acid deficiency. Given the role of glutamine metabolism in immune responses to *A fumigatus*, glutamine

Table 1. Demographics of the patients with CGD

								Series 1		Series 2		Series 3	Series 4		Series 5	
CGD	Age at the time of the first exp.	Sex	Mutation	History of inflammatory/ infectious complications	Active infection or inflammation event at the time of exp.? (if so which exp series)	Autoimmune phenotype?	IFN-γ therapy at the time of exp.?	Other medications	ELISA mono and neutro, proteome mono and neutro, SH mono	ATAC-seq and bulk RNA-seq mono	Training mono, mtROS neutro, SH neutro, metabolites neutro and mono	SH mono ± metformin	SH mono and training mono ± r-IFN-γ	SH mono ± r-IFN-γ, ELISA mono ± r-IFN-γ	scRNA-seq (data set 2) ± IFN-γ *ex vivo*	SH mono and PMN ± r-IFN-γ; ELISA PMN and trained mono ± r-IFN-γ	scRNA-seq (data set 3) in vivo IFN-γ treatment and ± IFN-γ *ex vivo*
A	39	M	AR p47^{phox} (*NCF1*) - homozygous 2-bp deletion	Invasive aspergillosis, IBD	No	No	No	Posaconazole, cotrimoxazole	Yes	Yes	Yes	No	Yes	No	No	Yes (± IFN-γ in vitro)	Yes ± IFN-γ ex vivo TruCulture
B	36	M	AR p47^{phox} (*NCF1*) - homozygous 2-bp deletion	Aspergillus and non-aspergillus-related inflammatory events (eg, liver abscess, acne)	Series 1: *S aureus* liver abscess being treated with flucloxacillin.	No	No	Posaconazole, cotrimoxazole	Yes	Yes	Yes	No	No	No	No	No	No
C	48	M	X-linked gp91^{phox} (*CYBB*) -intron 7 substitution at position +2 T>A, causing splicing defect, missing exon 7 in encoding mRNA	IBD, aphthous lesions	No	No	No	Posaconazole, cotrimoxazole, prednisolone	Yes	Yes	No	No	No	Yes	No	No	No
D	18	M	AR p47^{phox} (*NCF1*) - homozygous 2-bp deletion	Chilblain lupus, bacterial recurrent respiratory infections	No	Yes	No	Posaconazole, cotrimoxazole	Yes	Yes	Yes	Yes	Yes	Yes (only ELISA mono ± r-IFN-γ)	Yes (± IFN-γ ex vivo TruCulture)	No	No
E	18	M	AR p47^{phox} (*NCF1*) - homozygous 2-bp deletion	IBD, anti-dsDNA+, lymphadenitis	No	Yes	No	Posaconazole, cotrimoxazole, ustekinumab	Yes	Yes	Yes	No	No	Yes	No	No	No
F	27	F	AR p67^{phox} (*NCF2*) -C.879 C>G (p. (Tyr293*)	Chronic gingivitis, photocontact dermatitis	Series 4: pregnancy	No	No	Posaconazole, flucloxacillin	No	No	Yes	Yes	No	Yes	Yes (± IFN-γ ex vivo TruCulture)	No	No
G	28	M	AR p47^{phox} (*NCF1*) - homozygous 2-bp deletion	Invasive aspergillosis, hidradenitis	No	No	No	Posaconazole, cotrimoxazole	No	No	No	No	No	Yes	Yes (no + IFN-γ TruCulture)	No	No
H	30	M	X-linked gp91^{phox} (CYBB) -intronic insertion in intron 1 (extra STOP codon)	Invasive aspergillosis, IBD	No	No	No	Posaconazole, cotrimoxazole	No	No	No	No	No	Yes	Yes (± IFN-γ TruCulture)	No	No
I	42	M	X-linked gp91^{phox} (CYBB) -intronic insertion in intron 1 (extra STOP codon)	Invasive aspergillosis, bacterial and fungal recurrent respiratory infections	No	No	Yes	Itraconazole, cotrimoxazole	No	No	No	No	No	No	No	Yes ± IFN-γ ex vivo and in vivo before and after IFN-γ immunotherapy	Yes (before and after IFN-γ immunotherapy)

ELISA, enzyme-linked immunosorbent assay; F, female; IBD, inflammatory bowel disease; M, male; mtROS, mitochondrial ROS; PMN, polymorphonuclear neutrophils; SH, Seahorse.

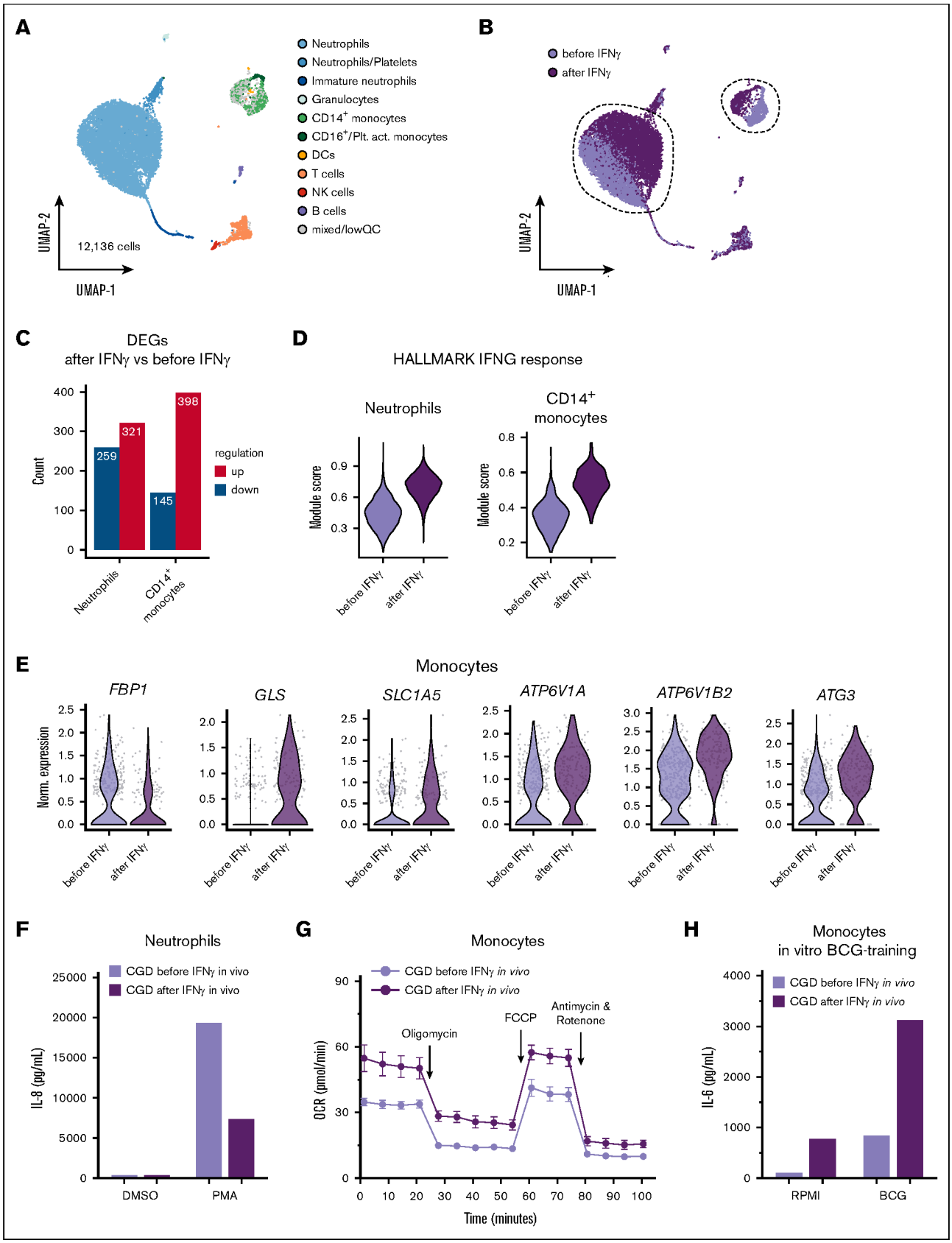
A
Neutrophils
Neutrophils/Platelets
Immature neutrophils
Granulocytes
CD14+ monocytes
CD16+/Plt. act. monocytes
DCs
T cells
NK cells
B cells
mixed/lowQC
12,136 cells
UMAP-2
UMAP-1
B
before IFNγ
after IFNγ
UMAP-2
UMAP-1
C
DEGs
after IFNγ vs before IFNγ
Count
regulation
up
down
259
321
145
398
Neutrophils
CD14+ monocytes
D
HALLMARK IFNG response
Neutrophils
CD14+ monocytes
Module score
before IFNγ
after IFNγ
E
Monocytes
FBP1
GLS
SLC1A5
ATP6V1A
ATP6V1B2
ATG3
Norm. expression
F
Neutrophils
CGD before IFNγ in vivo
CGD after IFNγ in vivo
IL-8 (pg/mL)
DMSO
PMA
G
Monocytes
CGD before IFNγ in vivo
CGD after IFNγ in vivo
Oligomycin
FCCP
Antimycin & Rotenone
OCR (pmol/min)
Time (minutes)
H
Monocytes
in vitro BCG-training
CGD before IFNγ in vivo
CGD after IFNγ in vivo
IL-6 (pg/mL)
RPMI
BCG

Figure 5.

deficiency in CGD monocytes may further impair fungal clearance and modulate cytokine responses.[40] Decreased amino acid levels have also been noted in chronic inflammation due to enhanced catabolism[19] in animal and human studies.[41,42] A similar mechanism may contribute to CGD pathophysiology. The defective induction of trained immunity observed in CGD may also reflect deficient glutamine metabolism.[30] In addition, reduced SDHB expression (part of ETC complex II) and intracellular α-KG levels in CGD monocytes point to mitochondrial dysfunction. The severe glycolytic impairment in CGD neutrophils might relate to a direct link between the NADPH complex and glycolysis, particularly 6-phosphofructo-2-kinase, previously described neutrophils.[43] Our findings challenge the classical view of neutrophils as predominantly glycolytic with low mitochondrial activity, revealing greater metabolic flexibility.[44] For instance, it has been found that they are capable of shifting from a primarily glycolytic state to one dominated by the oxidative pentose phosphate pathway, particularly in response to increased NADPH demand during oxidative burst.[45] Although the pentose phosphate pathway is not connected to mitochondrial metabolism, this evidence supports the broader concept that neutrophils can dynamically adapt their metabolic pathways depending on functional requirements. In the context of CGD, this plasticity might include an increased reliance on alternative energy sources, potentially involving mitochondrial metabolism, to compensate for impaired oxidative burst and altered glycolytic flux.

Prophylactic immunotherapy with IFN-γ has already been found to be effective in patients with CGD[12]; however, its precise mechanism remains unclear. Our study demonstrates that IFN-γ acts partly by metabolically rewiring innate immune cells, counteracting the pathological effects of NADPH oxidase deficiency, namely, exaggerated inflammation and impaired antifungal defense, particularly against *Aspergillus*. After IFN-γ incubation, monocytes from all patients with CGD exhibited increased ECAR and OCR, indicating partial restoration of intrinsic metabolic defects. This activation aligns with previous studies demonstrating the broad impact of IFN-γ on immune cell metabolism[46-49] and its role in promoting mitochondrial function of human monocytes by modulating the NAD^+ salvage pathway.[26] Moreover, IFN-γ upregulates *IDO1* expression,[50] potentially correcting dysregulated tryptophan metabolism in CGD,[27,51] thereby enhancing NAD^+ production through the kynurenine pathway and protecting tissues from *A fumigatus*–related immunopathology exacerbated by impaired indole 2,3-dioxygenase activity.[28] Functionally, IFN-γ rebalanced the excessive production of IL-6 and IL-1β on monocyte activation and boosted fungal killing of *Aspergillus* in 2 patients with CGD. We also captured in vivo evidence from a single patient with CGD undergoing IFN-γ therapy, in whom treatment led to increased mitochondrial metabolism and reduced IL-8 production by neutrophils, further supporting the involvement of metabolic reprogramming in the modulation of inflammatory responses. Together, these data reinforce the concept that metabolic reprogramming is a key effector mechanism of IFN-γ, even in the context of CGD.

Another finding was the defective capacity of CGD monocytes to mount a trained immunity response. Trained immunity is dependent on epigenetic modifications that are in turn dependent on metabolic rewiring.[30] Although we observed that CGD monocytes have altered chromatin accessibility, we could not identify an epigenetic signature that would clearly explain the defective trained immunity phenotype. Specifically, we found only a limited number of immune-related differentially accessible genes, such as *CLEC4C* (known also as BDCA2, which acts through Syk modulating type I IFN production in plasmacytoid dendritic cells[52]) and *NOX5* (a calcium-dependent NADPH oxidase, implicated in the differentiation into dendritic cells[53]). Other epigenetic mechanisms, such as histone modifications, DNA methylation, noncoding RNAs, and lactylation, might contribute to the hyperinflammatory phenotype and should be further investigated. Jacobs et al[54] have revealed that the addition of IFN-γ for 6 days boosted cytokine responses on restimulation in healthy volunteers. Similarly, the suppletion of IFN-γ restored the defective induction of trained immunity in patients with CGD both in vitro and in vivo. The increased expression of glutamine import (*SLC1A5*, known as *ASCT2*) and glutamine metabolism genes (*GLS*, *GLUL*) found in monocytes after the whole-blood ex vivo stimulation with IFN-γ in vitro could explain its additive effect on restoration of trained immunity in CGD and the boosted antifungal innate immune response.[30,40] Interestingly, IFN-γ enhanced trained immunity responses in CGD monocytes, whereas a modest reduction was observed in healthy controls. In CGD monocytes, which have impaired ROS-dependent signaling and metabolic dysfunction, IFN-γ may support trained immunity by promoting glutamine metabolism and increasing NAD^+ availability. In contrast, in healthy monocytes with intact metabolism, IFN-γ may trigger regulatory pathways that prevent excessive immune activation. Moreover, the aberrant trained immunity observed in CGD cells and its restoration by IFN-γ might reflect the distinct metabolic and functional activation states of these cells and the capacity of IFN-γ to modulate transcriptional responses and immune activation in these cells as previously reported.[55,56]

An important limitation of our study is the small sample size for certain analyses, which necessitates interpreting these specific findings as trends rather than definitive conclusions. In addition,

Figure 5. IFN-γ in vivo treatment leads to transcriptional reprogramming of cells and restores functional immunometabolic defects in monocytes from 1 patient with CGD. (A) uniform manifold approximation and projection (UMAP) visualization of 12 136 whole blood cells of 1 patient with CGD before and 4 hours after in vivo Imukine (rIFN-γ) subcutaneous treatment (50 mg/m^2 body surface area, with a maximum of 100 mg) profiled with scRNA-seq and colored by cell type. (B) UMAP visualization of cells colored by condition, before (light purple) and 4 hours after (dark purple) in vivo Imukine (rIFN-γ) treatment. (C) Numbers of differentially expressed genes identified as upregulated (red) or downregulated (blue) in neutrophils and $CD14^+$ monocytes. (D) Module score of the HALLMARK gene set "interferon gamma response" in neutrophils and $CD14^+$ monocytes before and after rIFN-γ treatment. (E) Violin plots of selected differentially expressed genes in $CD14^+$ monocytes isolated before and after in vivo rIFN-γ treatment. (F) IL-8 production after 4 hours of stimulation with either medium or PMA (50 ng/mL) in neutrophils from a patient with CGD before and 4 hours after receiving in vivo Imukine (rIFN-γ) subcutaneously. (G) OCR after Mito Stress Test of monocytes isolated from a patient with CGD before and 4 hours after receiving in vivo Imukine (rIFN-γ) subcutaneously. (H) IL-6 production from monocytes after LPS restimulation at day 6 after BCG-training protocol. Monocytes were isolated from 1 patient with CGD before and 4 hours after receiving Imukine (rIFN-γ). Owing to the low number of subjects, statistical analysis could not be performed for this set of experiments. DCs, dendritic cells; DMSO, dimethyl sulfoxide; NK, natural killer; Plt.act., platelet-activated; QC, quality control.

we were only able to study the in vivo effects of IFN-γ therapy in a single patient. Although IFN-γ therapy is beneficial for many patients with CGD, its utilization has been tempered due to frequent side effects and its complex immunomodulatory nature, highlighting the need for a more nuanced approach to select the subset of patients that will most likely benefit from the treatment. We observed that the global rIFN-γ–dependent transcriptional rewiring in patients with CGD is characterized by upregulation of key genes for antimicrobial host responses and downregulation of many genes coding for proinflammatory cytokines and chemokines. However, in 1 patient with CGD with an autoimmune phenotype (CGD D), increased expression of type I IFN-related genes and immune regulators after rIFN-γ ex vivo was observed. This upregulation could potentially exacerbate clinical features in patients with CGD with lupus-like disorders,[57] suggesting caution when considering rIFN-γ immunotherapy for this specific subgroup. We suggest implementing transcriptional or functional screening using in vitro cells from patients to assess individual responses to IFN-γ therapy. This approach could help identify patients with CGD who would benefit most from IFN-γ immunotherapy, allowing for more targeted and effective treatment approaches tailored to each patient's specific condition.

Our findings of the immunomodulatory effects of IFN-γ immunotherapy on dysregulated metabolism in patients with CGD do not stand alone. We previously observed that immunoparalysis in sepsis is linked to broad metabolic defects and that IFN-γ partially restored the metabolic status and the capacity to produce proinflammatory cytokines.[49] Exploring metabolic defects underlying diseases associated with immune dysregulation could open up novel insights into disease pathogenesis and might open doors for efficient and targeted immunotherapy with IFN-γ or other immunomodulatory treatments that target metabolism. In conclusion, we have identified a novel mechanism by which IFN-γ prophylaxis can exert its beneficial effect in patients with CGD and which could guide the development and exploration of immunotherapeutic strategies in diseases associated with severe infection and immune dysregulation.

Acknowledgments

The authors thank all healthy volunteers for donating blood. The authors thank Medeea Badii, Simone J.C.F.M. Moorlag, Priya A. Debisarun, Maartje Cleophas-Jacobs, Malin Ostman, Julia van Heck, and Intan M. Dewi for the logistical and experimental support; and Athanasios Ziogas for the suggestions regarding the setup of the experiments with apocynin.

F.L.v.d.V. was supported by a Vidi grant of the Netherlands Association for Scientific Research, the Europeans Union's Horizon 2020 research and innovation program under grant agreement number 847507 (HDM-FUN), and the "la Caixa" Foundation and Fundação para a Ciência e a Tecnologia (FCT) under the agreement LCF/PR/HR17/52190003 (TRANS-CPA). A.C. and C.C. were supported by FCT through the grants UIDB/50026/2020, UIDP/50026/2020, LA/P/0050/2020, PTDC/MED-OUT/1112/2021 to A.C. and CEECIND/04058/2018 and 2022.06674.PTDC to C.C., the "la Caixa" Foundation under the agreement LCF/PR/HR22/52420003 (MICROFUN) to C.C., and the "la Caixa" Foundation and FCT under the agreement LCF/PR/HR17/52190003 (TRANS-CPA) to A.C. A.V.F. is supported by the Fundo Sucial Europeu and FCT (PhD grant PD/BD/135449/2017). V.K. and R.J.R. were supported by Radboudumc personal PhD grants. L.A.B.J. was supported by a Samenwerkende Gezondheidsfondsen grant (TIMID) number A18-1432. M.G.N. was supported by an ERC Advanced Grant (number 833247) and a Spinoza Grant of the Netherlands Organization for Scientific Research. The work was supported by the German Research Foundation (DFG) to A.C.A. via grant number 458854699 and to J.L.S. under Germany's Excellence Strategy (EXC2151-390873048), as well as by the EU project DiscovAIR (grant number 874656) and the EU project SYSCID (grant number 733100). Y.L. was supported by an ERC Starting Grant (948207) and the Radboud University Medical Centre Hypatia grant (2018) for Scientific Research. N.v.R. was supported by the Wellcome Trust (grant number 226408/Z/22/Z).

Authorship

Contribution: M. Bruno, M.G.N., A.C., and F.L.v.d.V. conceived the study; M. Bruno, C.K., A.V.F., C.B., L.A.B.J., J.L.S., M.G.N., A.C.A., A.C., and F.L.v.d.V. designed the study and experiments; M. Bruno, A.V.F., C.K., R.J.R., R.L., C.I.v.d.M., L.G., V.K., N.A.F.J., D.R., H.T., J.S., C.G.-R., M.v.U., K.H., J.S.-S., L.B., S.M., H.J.F., M.K., M.S., and O.I.G. performed the experiments; C.K., B.Z., R.J.R., R.L., N.v.R., W.L., J.S., C.G.-R., M.v.U., A.A., S.M., H.J.F., S.W.-H., M. Becker, L.H., M.K., J.S.-S., L.B., K.H., C.C., M.S., J.L.S., Y.L., and A.C.A. contributed to bioinformatics analysis; M. Bruno, C.K., A.V.F., B.Z., R.J.R., R.L., C.I.v.d.M., N.v.R., L.G., V.K., A.A., C.C., J.L.S., L.A.B.J., C.B., M.G.N., Y.L., A.C.A., A.C., and F.L.v.d.V. interpreted the data; C.C., J.L.S., L.A.B.J., C.B., M.G.N., Y.L., A.C.A., A.C., and F.L.v.d.V. contributed to supervision; M. Bruno and F.L.v.d.V. wrote the initial draft; and all authors edited the final version.

Conflict-of-interest disclosure: M.S. was the inventor of the TruCulture technology and is the CEO of HOT Screen GmbH, the company that manufactures TruCulture. The remaining authors declare no competing financial interests.

ORCID profiles: M. Bruno, 0000-0002-5353-7691; C.K., 0000-0002-6627-3728; A.V.F., 0000-0002-6274-0448; B.Z., 0000-0002-2911-9422; R.J.R., 0000-0003-3921-7541; R.L., 0000-0001-9663-1357; C.I.v.d.M., 0000-0003-0763-4017; N.v.R., 0000-0001-6722-2757; N.A.F.J., 0000-0002-9629-8627; A.A., 0000-0003-1770-1332; H.T., 0000-0002-5988-6147; O.I.G., 0000-0002-4726-915X; S.M., 0000-0002-9885-4850; S.W.-H., 0000-0002-0890-5774; M. Becker, 0000-0002-7120-4508; L.B., 0000-0001-9675-7208; K.H., 0000-0001-5273-5277; J.L.S., 0000-0003-2812-9853; L.A.B.J., 0000-0001-6166-9830; C.B., 0000-0003-4722-491X; Y.L., 0000-0003-4022-7341; A.C.A., 0000-0002-9429-5457; A.C., 0000-0001-8935-8030.

Correspondence: Mariolina Bruno, Department of Internal Medicine and Radboudumc Community for Infectious Diseases, Radboud University Medical Center, Geert Grooteplein Zuid 10, 6526 GA Nijmegen, The Netherlands; email: mariolina.bruno@radboudumc.nl; and Frank L. van de Veerdonk, Department of Internal Medicine and Radboudumc Community for Infectious Diseases, Radboud University Medical Center, Geert Grooteplein Zuid 10, 6526 GA Nijmegen, The Netherlands; email: frank.vandeveerdonk@radboudumc.nl.

References

1. Giardino G, Cicalese MP, Delmonte O, et al. NADPH oxidase deficiency: a multisystem approach. *Oxid Med Cell Longev*. 2017;2017:4590127.
2. Moghadam ZM, Henneke P, Kolter J. From flies to men: ROS and the NADPH oxidase in phagocytes. *Front Cell Dev Biol*. 2021;9:628991.
3. Singel KL, Segal BH. NOX2-dependent regulation of inflammation. *Clin Sci*. 2016;130(7):479-490.
4. Schuett J, Schuett H, Oberoi R, et al. NADPH oxidase NOX2 mediates TLR2/ 6-dependent release of GM-CSF from endothelial cells. *The FASEB J*. 2017;31(6):2612-2624.
5. Seger RA. Chronic granulomatous disease 2018: advances in pathophysiology and clinical management. *LymphoSign J*. 2019;6(1):1-16.
6. van de Veerdonk FL, Smeekens SP, Joosten LAB, et al. Reactive oxygen species-independent activation of the IL-1 inflammasome in cells from patients with chronic granulomatous disease. *Proc Natl Acad Sci U S A*. 2010;107(7):3030-3033.
7. de Luca A, Smeekens SP, Casagrande A, et al. IL-1 receptor blockade restores autophagy and reduces inflammation in chronic granulomatous disease in mice and in humans. *Proc Natl Acad Sci USA*. 2014;111(9):3526-3531.
8. Roos D. Chronic granulomatous disease. *Br Med Bull*. 2016;118(1):50-63.
9. Cole T, Pearce MS, Cant AJ, Cale CM, Goldblatt D, Gennery AR. Clinical outcome in children with chronic granulomatous disease managed conservatively or with hematopoietic stem cell transplantation. *J Allergy Clin Immunol*. 2013;132(5):1150-1155.
10. Kohn DB, Booth C, Kang EM, et al. Lentiviral gene therapy for X-linked chronic granulomatous disease. *Nat Med*. 2020;26(2):200-206.
11. Marciano BE, Wesley R, De Carlo ES, et al. Long-term interferon-γ therapy for patients with chronic granulomatous disease. *Clin Infect Dis*. 2004;39 (5):692-699.
12. International Chronic Granulomatous Disease Cooperative Study Group. A controlled trial of interferon gamma to prevent infection in chronic granulomatous disease. *N Engl J Med*. 1991;324(8):509-516.
13. Avau A, Matthys P. Therapeutic potential of interferon-γ and its antagonists in autoinflammation: lessons from murine models of systemic juvenile idiopathic arthritis and macrophage activation syndrome. *Pharmaceuticals (Basel)*. 2015;8(4):793-815.
14. Cirovic B, de Bree LCJ, Groh L, et al. BCG vaccination in humans elicits trained immunity via the hematopoietic progenitor compartment. *Cell Host Microbe*. 2020;28(2):322-334.e5.
15. Wickham H, Grolemund G. In: *R for Data Science: Import, Tidy, Transform, Visualize, and Model Data*. 1st ed. O'Reilly; 2016.
16. Domínguez-Andrés J, Arts RJW, Bekkering S, et al. *In vitro* induction of trained immunity in adherent human monocytes. *STAR Protoc*. 2021;2(1): 100365.
17. Bylund J, MacDonald KL, Brown KL, et al. Enhanced inflammatory responses of chronic granulomatous disease leukocytes involve ROS-independent activation of NF-κB. *Eur J Immunol*. 2007;37(4):1087-1096.
18. Smeekens SP, Henriet SSV, Gresnigt MarkS, et al. Low interleukin-17A production in response to fungal pathogens in patients with chronic granulomatous disease. *J Interferon Cytokine Res*. 2012;32(4):159-168.
19. Zhu X, Meyers A, Long D, et al. Frontline science: monocytes sequentially rewire metabolism and bioenergetics during an acute inflammatory response. *J Leukoc Biol*. 2019;105(2):215-228.
20. Mafi S, Mansoori B, Taeb S, et al. mTOR-mediated regulation of immune responses in cancer and tumor microenvironment. *Front Immunol*. 2021;12: 774103.
21. Liu F, Fan LM, Michael N, Li JM. In vivo and in silico characterization of apocynin in reducing organ oxidative stress: a pharmacokinetic and pharmacodynamic study. *Pharmacol Res Perspect*. 2020;8(4):e00635.
22. Ramsey IS, Ruchti E, Kaczmarek JS, Clapham DE. Hv1 proton channels are required for high-level NADPH oxidase-dependent superoxide production during the phagocyte respiratory burst. *Proc Natl Acad Sci U S A*. 2009;106(18):7642-7647.
23. Lachmandas E, Eckold C, Böhme J, et al. Metformin alters human host responses to mycobacterium tuberculosis in healthy subjects. *J Infect Dis*. 2019;220(1):139-150.
24. Bharath LP, Agrawal M, McCambridge G, et al. Metformin enhances autophagy and normalizes mitochondrial function to alleviate aging-associated inflammation. *Cell Metab*. 2020;32(1):44-55.e6.
25. Keating ST, Groh L, Thiem K, et al. Rewiring of glucose metabolism defines trained immunity induced by oxidized low-density lipoprotein. *J Mol Med*. 2020;98(6):819-831.
26. McCann KJ, Christensen SM, Colby DH, et al. IFNγ regulates NAD+ metabolism to promote the respiratory burst in human monocytes. *Blood Adv*. 2022;6(12):3821-3834.
27. Romani L, Fallarino F, De Luca A, et al. Defective tryptophan catabolism underlies inflammation in mouse chronic granulomatous disease. *Nature*. 2008;451(7175):211-215.
28. Zelante T, Choera T, Beauvais A, et al. Aspergillus fumigatus tryptophan metabolic route differently affects host immunity. *Cell Rep*. 2021;34(4): 108673.
29. Choera T, Zelante T, Romani L, Keller NP. A Multifaceted role of tryptophan metabolism and indoleamine 2,3-dioxygenase activity in aspergillus fumigatus–host interactions. *Front Immunol*. 2017;8:1996.

30. Arts RJW, Novakovic B, ter Horst R, et al. Glutaminolysis and fumarate accumulation integrate immunometabolic and epigenetic programs in trained immunity. *Cell Metab*. 2016;24(6):807-819.

31. Adane B, Ye H, Khan N, et al. The hematopoietic oxidase NOX2 regulates self-renewal of leukemic stem cells. *Cell Rep*. 2019;27(1):238-254.e6.

32. Henriquez-Olguin C, Meneses-Valdes R, Raun SH, et al. NOX2 deficiency exacerbates diet-induced obesity and impairs molecular training adaptations in skeletal muscle. *Redox Biol*. 2023;65:102842.

33. Ijurko C, Romo-González M, García-Calvo C, et al. NOX2 control over energy metabolism plays a role in acute myeloid leukaemia prognosis and survival. *Free Radic Biol Med*. 2023;209:18-28.

34. Monjarret B, Shour S, Benyoucef A, et al. NOX2 deficiency enhances priming and activation of the NLRP3 inflammasome. *J Allergy Clin Immunol*. Published online 5 October 2023. https://doi.org/10.1016/j.jaci.2023.09.030

35. Brown KL, Bylund J, MacDonald KL, et al. ROS-deficient monocytes have aberrant gene expression that correlates with inflammatory disorders of chronic granulomatous disease. *Clin Immunol*. 2008;129(1):90-102.

36. Kobayashi SD, Voyich JM, Braughton KR, et al. Gene expression profiling provides insight into the pathophysiology of chronic granulomatous disease. *J Immunol*. 2004;172(1):636-643.

37. McLetchie S, Volpp BD, Dinauer MC, Blum JS. Hyper-responsive Toll-like receptor 7 and 9 activation in NADPH oxidase-deficient B lymphoblasts. *Immunology*. 2015;146(4):595-606.

38. Meissner F, Seger RA, Moshous D, Fischer A, Reichenbach J, Zychlinsky A. Inflammasome activation in NADPH oxidase defective mononuclear phagocytes from patients with chronic granulomatous disease. *Blood*. 2010;116(9):1570-1573.

39. O'Neill LAJ, Kishton RJ, Rathmell J. A guide to immunometabolism for immunologists. *Nat Rev Immunol*. 2016;16(9):553-565.

40. Antunes D, Gonçalves SM, Matzaraki V, et al. Glutamine metabolism supports the functional activity of immune cells against aspergillus fumigatus. *Microbiol Spectr*. 2023;11(1):e0225622.

41. Mercier S, Breuillé D, Mosoni L, Obled C, Patureau Mirand P. Chronic inflammation alters protein metabolism in several organs of adult rats. *J Nutr*. 2002;132(7):1921-1928.

42. Suliman ME, Qureshi AR, Stenvinkel P, et al. Inflammation contributes to low plasma amino acid concentrations in patients with chronic kidney disease. *Am J Clin Nutr*. 2005;82(2):342-349.

43. Baillet A, Hograindleur MA, El Benna J, et al. Unexpected function of the phagocyte NADPH oxidase in supporting hyperglycolysis in stimulated neutrophils: key role of 6-phosphofructo-2-kinase. *FASEB J*. 2017;31(2):663-673.

44. Kumar S, Dikshit M. Metabolic insight of neutrophils in health and disease. *Front Immunol*. 2019;10:2099.

45. Britt EC, Lika J, Giese MA, et al. Switching to the cyclic pentose phosphate pathway powers the oxidative burst in activated neutrophils. *Nat Metab*. 2022;4(3):389-403.

46. Jessop F, Buntyn R, Schwarz B, Wehrly T, Scott D, Bosio CM. Interferon gamma reprograms host mitochondrial metabolism through inhibition of complex II to control intracellular bacterial replication. *Infect Immun*. 2020;88(2):e00744-19.

47. Su X, Yu Y, Zhong Y, et al. Interferon-γ regulates cellular metabolism and mRNA translation to potentiate macrophage activation. *Nat Immunol*. 2015;16(8):838-849.

48. Kiritsy MC, McCann K, Mott D, et al. Mitochondrial respiration contributes to the interferon gamma response in antigen-presenting cells. *eLife*. 2021;10:e65109.

49. Cheng SC, Scicluna BP, Arts RJW, et al. Broad defects in the energy metabolism of leukocytes underlie immunoparalysis in sepsis. *Nat Immunol*. 2016;17(4):406-413.

50. Mellor AL, Lemos H, Huang L. Indoleamine 2,3-dioxygenase and tolerance: where are we now? *Front Immunol*. 2017;8:1360.

51. Romani L, Puccetti P. Romani & puccetti reply. *Nature*. 2014;514(7523):E18.

52. Riboldi E, Daniele R, Parola C, et al. Human C-type lectin domain family 4, member C (CLEC4C/BDCA-2/CD303) is a receptor for asialo-galactosyl-oligosaccharides. *J Biol Chem*. 2011;286(41):35329-35333.

53. Marzaioli V, Hurtado-Nedelec M, Pintard C, et al. NOX5 and p22phox are 2 novel regulators of human monocytic differentiation into dendritic cells. *Blood*. 2017;130(15):1734-1745.

54. Jacobs MME, Maas RJF, Jonkman I, et al. Trained immunity is regulated by T cell-induced CD40-TRAF6 signaling. *Cell Rep*. 2024;43(9):114664.

55. Frazão JB, Colombo M, Simillion C, et al. Gene expression in chronic granulomatous disease and interferon-γ receptor deficient cells treated in vitro with interferon-γ. *J Cell Biochem*. 2019;120(3):4321-4332.

56. Fernandez-Boyanapalli R, McPhillips KA, Frasch SC, et al. Impaired phagocytosis of apoptotic cells by macrophages in chronic granulomatous disease is reversed by IFN-γ in a nitric oxide-dependent manner. *J Immunol*. 2010;185(7):4030-4041.

57. Cale CM, Morton L, Goldblatt D. Cutaneous and other lupus-like symptoms in carriers of X-linked chronic granulomatous disease: incidence and autoimmune serology. *Clin Exp Immunol*. 2007;148(1):79-84.